

Evaluation of population structure inferred by principal component analysis or the admixture model

Jan van Waaij^{1,3,†}, Song Li^{1,†}, Genís Garcia-Erill², Anders Albrechtsen² and Carsten Wiuf^{1,*}

¹Department of Mathematical Science, University of Copenhagen, 2100 Copenhagen, Denmark

²Department of Biology, University of Copenhagen, 2100 Copenhagen, Denmark

³Current address: Department of Health Technology, Danish Technical University, 2800 Kgs. Lyngby, Denmark

[†]These authors contributed equally to this work

*Corresponding author: Department of Mathematical Sciences, Universitetsparken 5, 2100 Copenhagen, Denmark. Email: wiuf@math.ku.dk

Abstract

Principal component analysis (PCA) is commonly used in genetics to infer and visualize population structure and admixture between populations. PCA is often interpreted in a way similar to inferred admixture proportions, where it is assumed that individuals belong to one of several possible populations or are admixed between these populations. We propose a new method to assess the statistical fit of PCA (interpreted as a model spanned by the top principal components) and to show that violations of the PCA assumptions affect the fit. Our method uses the chosen top principal components to predict the genotypes. By assessing the covariance (and the correlation) of the residuals (the differences between observed and predicted genotypes), we are able to detect violation of the model assumptions. Based on simulations and genome wide human data we show that our assessment of fit can be used to guide the interpretation of the data and to pinpoint individuals that are not well represented by the chosen principal components. Our method works equally on other similar models, such as the admixture model, where the mean of the data is represented by linear matrix decomposition.

Keywords: PCA; residuals; population modelling; ancient DNA; statistical fit

Introduction

Principal component analysis (PCA) and model-based clustering methods are popular ways to disentangle the ancestral genetic history of individuals and populations. One particular model, the admixture model (Pritchard *et al.* 2000), has played a prominent role because of its simple structure and, in some cases, easy interpretability. PCA is often seen as being model free but as noted by Engelhardt and Stephens (2010), the two approaches are very similar. The interpretation of the results of a PCA analysis is often based on assumptions similar to those of the admixture model, such that admixed individuals are linear combinations of the eigenvectors representing unadmixed individuals. In this way, the admixed individuals lie in-between the unadmixed individuals in a PCA plot. As shown for the admixture model, there are many demographic histories that can lead to the same result (Lawson *et al.* 2018a) and many demographic histories that violate the assumptions of the admixture model (Garcia-Erill and Albrechtsen 2020). As we will show, this is also the case for PCA, since it has a similar underlying model (Engelhardt and Stephens 2010).

The admixture model states that the genetic material from each individual is composed of contributions from k distinct ancestral homogeneous populations. However, this is often contested in real data analysis, where the ancestral population structure might be much more complicated than that specified by the admixture model. For example, the k ancestral populations might be heterogeneous themselves, the exact number of ancestral populations might be difficult to assess due to many smaller contributing populations, or the genetic composition of an individual might be the result of continuous migration or recent

backcrossing, which also violates the assumptions of the admixture model. Furthermore, the admixture model assumes individuals are unrelated, which naturally might not be the case. This paper is concerned with assessing the fit of PCA building on the special relationship with the admixture model (Engelhardt and Stephens 2010). In particular, we are interested in quantifying the model fit and assessing the validity of the model at the level of the sample as well as at the level of the individual. Using real and simulated data we show that the fit from a PCA analysis is affected by violations of the admixture model.

We consider genotype data G from n individuals and m SNPs, such that $G_{si} \in \{0, 1, 2\}$ is the number of reference alleles for individual i and SNP s . Typically, G_{si} is assumed to be binomially distributed with parameter Π_{si} , where Π_{si} depends on the number of ancestral populations, k , their admixture proportions and the ancestral population allele frequencies. For clustering based analysis such as ADMIXTURE (Alexander and Lange 2011), k is the number of clusters while in PCA, it is the $k - 1$ top principal components. We give the specifics of the admixture model in the next section and show its relationship to PCA in the Material and methods section.

Several methods aim to estimate the best k in some sense (Alexander and Lange 2011; Evanno *et al.* 2005; Pritchard *et al.* 2000; Raj *et al.* 2014; Wang 2019), but finding such k does not imply the data fit the model (Lawson *et al.* 2018b; Janes *et al.* 2017). In statistics, it is standard to use residuals and distributional summaries of the residuals to assess model fit (Box *et al.* 2005). The residual of an observation is defined as the difference between the observed and the predicted value (estimated under some model). Visual trends in the residuals (for example, differences between populations) are indicative of model

misfit, and large absolute values of the residuals are indicative of outliers (for example due to experimental errors, or kinship). If the model is correct, a histogram of the residuals is expected to be unimodal centered around zero (Box *et al.* 2005).

In our context, Garcia-Erill and Albrechtsen (2020) argue that trends in the residual correlation matrix carries information about the underlying model and might be used for visual model evaluation. A method is designed to assess whether the correlation structure agrees with the proposed model, in particular, whether it agrees with the proposed number of homogeneous ancestral populations (Garcia-Erill and Albrechtsen 2020). However, even in the case the model is correctly specified, the residuals are in general correlated (Box *et al.* 2005), and therefore, trends might be observed even if the model is true, leading to incorrect model assessment. To adjust for this correlation, a leave-one-out procedure, based on maximum likelihood estimation of the admixture model parameters, is developed that removes the correlation between residuals in the case the model is correct, but not if the model is misspecified (Garcia-Erill and Albrechtsen 2020). This approach could also be applied to PCA, where expected genotypes could be calculated using probabilistic PCA (Meisner *et al.* 2021). This leave-one-out procedure is, however, computationally expensive.

To remedy the computational difficulties, we take a different approach to investigate the correlation structure. We suggest two different ways of calculating the correlation matrix of the residuals. The first is simply the empirical correlation matrix of the residuals. The second might be considered an estimated correlation matrix, based on a model. Both are simple to compute. Under mild regularity assumptions, these two measures agree if the model is correct and the number of SNPs is large. Hence, their difference is expected to be close to zero, when the admixture model is not violated. If the difference is considerably different from zero, then this is proof of model misfit.

To explore the adequacy of the proposed method, we investigate different ways to calculate the predicted values of the genotype (hence, the residuals), using Principal Component Analysis (PCA) in different ways. However, we also show that this approach can be used on estimated admixture proportions. Specifically, we use 1) an uncommon but very useful PCA approach (here, named PCA 1) based on unnormalized genotypes (Cabreros and Storey 2019; Chen and Storey 2015), 2) PCA applied to mean centred data (PCA 2), see Patterson *et al.* (2006), and 3) PCA applied to mean and variance normalised data (PCA 3) (Patterson *et al.* 2006). All three approaches are computationally fast and do not require separate estimation of ancestral allele frequencies and population proportions, as in Garcia-Erill and Albrechtsen (2020). Hence, the computation of the residuals are computationally inexpensive. Additionally, we show that this approach can also be applied to output from, for example, the software ADMIXTURE (Alexander *et al.* 2009) to estimate Π_{si} for each s and i , and to calculate the residuals from these estimates. An overview of PCA can be found in Jolliffe and Cadima (2016).

We demonstrate that our proposed method works well on simulated and real data, when the predicted values (and the residuals) are calculated in any of the four mentioned ways. Furthermore, we back this up mathematically by showing that the two correlation measures agree (if the number of SNPs is large) under the correct admixture model for PCA 1 and PCA 2. For the latter, a few additional assumptions are required. The estimated covariance (and correlation coefficient) under the proposed model might be seen as a correction term for population structure. Subtracting it from the empirical covariance, thus gives a covariance estimate with baseline zero under the correct model, independent of the population structure. It is natural to suspect that similar can be done in models with population structure and kinship, which we will pursue in a subsequent study.

In the next section, we describe the model, the statistical approach to compute the residuals, and how we evaluate model fit. In addition, we give mathematical statements that show how the method performs theoretically. In the ‘Results’ section, we provide analysis of simulated and real data, respectively. We end with a discussion. Mathematical proofs are collected in the appendix.

Materials and methods

Notation

For an $\ell_1 \times \ell_2$ matrix $A = (A_{ij})_{i,j}$, A_{*i} denotes the i -th column of A , A_{i*} the i -th row, A^T the transpose matrix, and $\text{rank}(A)$ the rank. The Frobenius norm of a square $\ell \times \ell$ matrix A is

$$\|A\|_F = \sqrt{\sum_{i=1}^{\ell} \sum_{j=1}^{\ell} A_{ij}^2}.$$

A square matrix A is an orthogonal projection if $A^2 = A$ and $A^T = A$. A symmetric matrix has n real eigenvalues (with multiplicity) and the eigenvectors can be chosen such that they are orthogonal to each other. If the matrix is positive (semi-)definite, then the eigenvalues are positive (non-negative).

For a random variable/vector/matrix X , its expectation is denoted $\mathbb{E}[X]$ (provided it exist). The variance of a random variable X is denoted $\text{var}(X)$, and covariance between two random variables X, Y is denoted $\text{cov}(X, Y)$ (provided they exist). Similarly, for a random vector $X = (X_1, \dots, X_n)$, the covariance matrix is denoted $\text{cov}(X)$. For a sequence X_m , $m = 0, \dots$, of random variables/vectors/matrices, if $X_m \rightarrow X_0$ as $m \rightarrow \infty$ almost surely (convergence for all realisations but a set of zero probability), we leave out ‘almost surely’ and write $X_m \rightarrow X_0$ as $m \rightarrow \infty$ for convenience.

The PCA and the admixture model

We consider a model with genotype observations from n individuals, and m biallelic sites (SNPs), where m is assumed to be (much) larger than n , $m \geq n$. The genotype G_{si} of SNP s in individual i is assumed to be a binomial random variable

$$G_{si} \sim \text{binomial}(2, \Pi_{si}).$$

In matrix notation, we have $G \sim \text{binomial}(2, \Pi)$ with expectation $\mathbb{E}(G | \Pi) = 2\Pi$, where G and Π are $m \times n$ dimensional matrices. Conditional on Π , we assume the entries of G are independent random variables.

Furthermore, we assume the matrix Π takes the form $\Pi = FQ$, where Q is a (possibly unconstrained) $k \times n$ matrix of rank $k \leq n$, and F is a (possibly unconstrained) $m \times k$ matrix, also of rank k (implying Π likewise is of rank k , Lemma 13). Entry-wise, this amounts to

$$\Pi_{si} = (FQ)_{si} = \sum_{k=1}^k F_{sk} Q_{ki}, \quad s = 1, \dots, m, \quad i = 1, \dots, n.$$

For the binomial assumption to make sense, we must require the entries of Π to be between zero and one.

In the literature, this model is typically encountered in the form of an admixture model with k ancestral populations, see for example, Pritchard *et al.* (2000); Garcia-Erill and Albrechtsen (2020). The general unconstrained setting which applies to PCA has also been discussed (Cabreros and Storey 2019). In the case of an admixture model, Q is a matrix of ancestral admixture proportions, such that the proportion of individual i 's genome originating from population j is Q_{ji} . Furthermore, F is a matrix of ancestral SNP frequencies, such

that the frequency of the reference allele of SNP s in population j is F_{sj} . In many applications, the columns of Q sum to one.

While we lean towards an interpretation in terms of ancestral population proportions and SNP frequencies, our approach does not enforce or assume the columns of Q (the admixture proportions) to sum to one, but allow these to be unconstrained. This is advantageous for at least two reasons. First, a proposed model might only contain the major ancestral populations, leaving out older or lesser defined populations. Hence, the sum of ancestral proportions might be smaller than one. Secondly, when fitting a model with fewer ancestral populations than the true model, one should only require the admixture proportions to sum to at most one.

The residuals

Our goal is to design a strategy to assess the hypothesis that Π is a product of two matrices. As we do not know the true k , we suggest a number k' of ancestral populations and estimate the model parameters under this constraint. That is, we assume a model of the form

$$G \sim \text{binomial}(2, \Pi_{k'}), \quad \Pi_{k'} = F_{k'} Q_{k'},$$

where each entry of G follows a binomial distribution. $Q_{k'}$ has dimension $k' \times n$, $F_{k'}$ has dimension $m \times k'$, and $\text{rank}(Q_{k'}) = \text{rank}(F_{k'}) = k'$, hence also $\text{rank}(\Pi_{k'}) = k'$. Throughout, we use the index k' to indicate the imposed rank condition, and assume $k' \leq k$ unless otherwise stated. The latter assumption is only to guarantee the mathematical validity of certain statements, and is not required for practical use of the method.

Our approach is build on the residuals, the difference between observed and predicted data. To define the residuals, we let $P: \mathbb{R}^n \rightarrow \mathbb{R}^n$ be the orthogonal projection onto the k -dimensional subspace spanned by the k rows of (the true) Q , hence $P = Q^T(QQ^T)^{-1}Q$, and $QP = Q$. Let $\hat{P}_{k'}$ be an estimate of P based on the data G , and assume $\hat{P}_{k'}$ is an orthogonal projection onto a k' -dimensional subspace. Later in this section, we show how an estimate $\hat{P}_{k'}$ can be obtained from an estimate of $Q_{k'}$ or an estimate of $\Pi_{k'}$. Estimates of these parameters might be obtained using existing methods, based on for example, maximum likelihood analysis (Wang 2003; Alexander et al. 2009; Garcia-Erill and Albrechtsen 2020). Furthermore, for the three PCA approaches, an estimate of the projection matrix can simply be obtained from eigenvectors of a singular value decomposition (SVD) of the data matrix.

We define the $m \times n$ matrix of residuals by

$$R_{k'} = G - 2\hat{\Pi} = G(I - \hat{P}_{k'}),$$

where G is the observed data and $G\hat{P}_{k'}$, the predicted values. The latter might also be considered an estimate of 2Π , the expected value of G . This definition of residuals is in line with how the residuals are defined in a multilinear regression model as the difference between the observed data (here, G) and the projection of the data onto the subspace spanned by the regressors (here, $G\hat{P}_{k'}$). The essential difference being that in a multilinear regression model, the regressors are known and does not depend on the observed data, while $\hat{P}_{k'}$ is estimated from the data.

We assess the model fit by studying the correlation matrix of the residuals in two ways. First, we consider the *empirical covariance matrix* \hat{B} with entries

$$\begin{aligned} \hat{B}_{ij} &= \frac{1}{m-1} \sum_{s=1}^m (R_{k',si} - \bar{R}_{k',i})(R_{k',sj} - \bar{R}_{k',j}) \\ &= \frac{1}{m-1} \sum_{s=1}^m (R_{k',si}R_{k',sj} - \bar{R}_{k',i}\bar{R}_{k',j}), \end{aligned}$$

where

$$\bar{R}_{k'i} = \frac{1}{m} \sum_{s=1}^m R_{k',si},$$

and the corresponding *empirical correlation matrix* with entries

$$\hat{b}_{ij} = \frac{\hat{B}_{ij}}{\sqrt{\hat{B}_{ii}\hat{B}_{jj}}},$$

$i, j = 1, \dots, n$. Secondly, we consider the *estimated covariance matrix*

$$\hat{C} = (I - \hat{P}_{k'})\hat{D}(I - \hat{P}_{k'})$$

with corresponding *estimated correlation matrix*,

$$\hat{c}_{ij} = \frac{\hat{C}_{ij}}{\sqrt{\hat{C}_{ii}\hat{C}_{jj}}},$$

$i, j = 1, \dots, n$. Here, \hat{D} is the $n \times n$ diagonal matrix containing the average heterozygosities of each individual,

$$\hat{D}_{ii} = \frac{1}{m} \sum_{s=1}^m G_{si}(2 - G_{si}), \quad i = 1, \dots, n.$$

Under reasonable regularity conditions, we can quantify the behaviour of \hat{B} and \hat{C} as the number of SNPs become large. Specifically, we assume the rows of F are independent and identically distributed with distribution $\text{Dist}(\mu, \Sigma)$, where μ denote the k -dimensional mean vector of the distribution, and Σ the $k \times k$ -covariance matrix, that is,

$$F_{s*} = (F_{s1}, \dots, F_{sk}) \stackrel{\text{iid}}{\sim} \text{Dist}(\mu, \Sigma),$$

$s = 1, \dots, m$. The matrix Q is assumed to be non-random, that is, fixed. These assumptions are standard and typically used in simulation of genetic data, see for example, Pickrell and Pritchard (2012); Cabrer0s and Storey (2019); Garcia-Erill and Albrechtsen (2020). Often $\text{dist}(\mu, \Sigma)$ is taken to be the product of k independent uniform distributions in which case $\mu = 0.5(1, 1, \dots, 1)$ and Σ is a diagonal matrix with entries $1/12$, though other choices have been applied, see for example Balding and Nichols (1995); Conomos et al. (2016).

Let D be the diagonal matrix with entries

$$D_{ii} = 2\mathbb{E}[\Pi_{si}(1 - \Pi_{si})], \quad i = 1, \dots, n. \quad (1)$$

It follows from Lemma 7 in the appendix, that \hat{D} converges to D as $m \rightarrow \infty$. Furthermore, as D_{ii} is the variance of G_{si} (it is binomial), then \hat{D}_{ii} might be considered an estimate of this variance. The proofs of the statements are in the appendix.

Theorem 1. *Let $k' \leq k$. Under the given assumptions, suppose further that $\hat{P}_{k'} \rightarrow P_{k'}$ as $m \rightarrow \infty$, for some matrix $P_{k'}$. Then, $P_{k'}$ is an orthogonal projection. Furthermore, the following holds,*

$$\begin{aligned} \hat{B} &\rightarrow (I - P_{k'})(D + 4Q^T\Sigma Q)(I - P_{k'}), \\ \hat{C} &\rightarrow (I - P_{k'})D(I - P_{k'}), \end{aligned}$$

as $m \rightarrow \infty$. Hence, also

$$\begin{aligned} \hat{B} - \hat{C} &\rightarrow 4(I - P_{k'})Q^T\Sigma Q(I - P_{k'}) \\ &= 4(P - P_{k'})Q^T\Sigma Q(P - P_{k'}), \end{aligned}$$

as $m \rightarrow \infty$. For $k' = k$, if $P_k = P$, then the right hand side is the zero matrix, whereas this is not the case in general for $k' < k$.

Theorem 2. *Assume $k' = k$ and $P_k = P$. Furthermore, suppose as in Theorem 1 and that the vector with all entries equal to one is in the space spanned by the rows of Q (this is, for example, the case if the admixture proportions sum to one for each individual). Then,*

$$\frac{\sum_{i=1}^n \sum_{j=1, i \neq j}^n \hat{B}_{ij}}{\sum_{i=1}^n \hat{B}_{ii}} \rightarrow -1, \quad \text{as } m \rightarrow \infty. \quad (2)$$

In addition, if Q takes the form

$$Q = \begin{pmatrix} Q_1 & 0 & \cdots & 0 \\ 0 & Q_2 & \cdots & 0 \\ \vdots & \vdots & \ddots & \vdots \\ 0 & 0 & \cdots & Q_r \end{pmatrix}$$

where Q_ℓ has dimension $k_\ell \times n_\ell$, $\sum_{\ell=1}^r k_\ell = k$ and $\sum_{\ell=1}^r n_\ell = n$, then (2) holds for each component of n_ℓ individuals. If $Q_\ell = (1 \dots 1)$, then

$$\hat{b}_{ij} \rightarrow -\frac{1}{n_\ell - 1}, \quad \text{as } m \rightarrow \infty,$$

for all individuals i, j in the ℓ -th component, irrespective the form of $Q_{\ell'}$, $\ell' \neq \ell$.

Theorem 3. Assume $k' = k$ and $P_k = P$. Furthermore, suppose as in Theorem 1 and that Q takes the form

$$Q = \begin{pmatrix} Q_1 & Q_2 \\ 0 & Q_3 \end{pmatrix},$$

where $Q_1 = (1 \dots 1)$ has dimension $1 \times n_1$, $n_1 \leq n$. Then, \hat{b}_{ij} converges as $m \rightarrow \infty$ to a value larger than or equal to $-\frac{1}{n_1 - 1}$, for all $i, j = 1, \dots, n_1$.

The same statements in the last two theorems hold with \hat{B} and \hat{b} replaced by \hat{C} and \hat{c} , respectively.

The three theorems provide means to evaluate the model. In particular, Theorem 1 might be used to assess the correctness (or appropriateness) of the proposed k' , while Theorem 2 and Theorem 3 might be used to assess whether data from a group of individuals (e.g., a modern day population) originates from a single ancestral population, irrespective, the origin of the remaining individuals. We give examples in the Results section.

The work flow is shown in Algorithm 1. We process real and simulated genotype data using PCA 1, PCA 2, PCA 3, and the software ADMIXTURE, and evaluate the fit of the model.

Algorithm 1 Work flow of the proposed method

1. Choose k' ,
2. Compute an estimate $\hat{P}_{k'}$ of the projection P ,
3. Calculate the residuals $R_{k'} = G(I - \hat{P}_{k'})$,
4. Calculate the correlation coefficients, \hat{b} and \hat{c} ,
5. Plot \hat{b} and the difference, the corrected correlation coefficients, $\hat{b} - \hat{c}$,
6. Assess visually the fit of the model.

Estimation of $P_{k'}$

Estimation of Q, F , and Π has received considerable interest in the literature, using for example, maximum likelihood (Wang 2003; Alexander et al. 2009), Bayesian approaches (Pritchard et al. 2000) or PCA (Engelhardt and Stephens 2010).

We discuss different ways to obtain an estimate $\hat{P}_{k'}$ of P .

Using an estimate $\hat{Q}_{k'}$ of $Q_{k'}$ An estimate $\hat{P}_{k'}$ might be obtained by projecting onto the subspace spanned by the k' rows of $\hat{Q}_{k'}$,

$$\hat{P}_{k'} = \hat{Q}_{k'}^T (\hat{Q}_{k'} \hat{Q}_{k'}^T)^{-1} \hat{Q}_{k'},$$

assuming $\text{rank}(\hat{Q}_{k'}) = k'$ for the calculation to be valid.

We apply this approach to estimate the projection matrix using output from the software ADMIXTURE.

Using an estimate $\hat{\Pi}_{k'}$ of $\Pi_{k'}$ Let $\tilde{\Pi}_{k'}$ be k' linearly independent rows chosen from $\hat{\Pi}_{k'}$ (out of m rows). Then, an estimate $\hat{P}_{k'}$ of $P_{k'}$ is

$$\hat{P}_{k'} = \tilde{\Pi}_{k'}^T (\tilde{\Pi}_{k'} \tilde{\Pi}_{k'}^T)^{-1} \tilde{\Pi}_{k'},$$

assuming $\text{rank}(\hat{\Pi}_{k'}) = k'$ for the calculation to be valid. Alternatively, one might apply the Gram-Schmidt method in which case the vectors are orthonormal by construction and $\hat{P}_{k'} = \tilde{\Pi}_{k'}^T \tilde{\Pi}_{k'}$. The estimate $\hat{P}_{k'}$ is independent of the choice of the k' rows, provided $\text{rank}(\hat{\Pi}_{k'}) = k'$.

Using PCA 1 We consider a PCA approach, originally due to Chen and Storey (2015), to estimate the space spanned by the rows of Q . We follow the procedure laid out in Cabrer0s and Storey (2019).

Let \hat{H} be the symmetric matrix

$$\hat{H} = \frac{1}{m} G^T G - \hat{D}.$$

Since \hat{H} is symmetric, all eigenvalues are real and the matrix is diagonalisable. Furthermore, \hat{H} is a variance adjusted version of $\frac{1}{m} G^T G$, see (1). Let $u_1, \dots, u_{k'}$ be $k' \leq k$ orthogonal eigenvectors belonging to the k' largest eigenvalues of \hat{H} , counted with multiplicities. Define the $n \times k'$ matrix $U_{k'} = (u_1, \dots, u_{k'})$ and the $n \times n$ orthogonal projection matrix

$$\hat{P}_{k'} = U_{k'} (U_{k'}^T U_{k'})^{-1} U_{k'}^T = U_{k'} U_{k'}^T$$

onto the subspace given by the span of the vectors $u_1, \dots, u_{k'}$.

In this particular case, convergence of $\hat{P}_{k'}$ can be made precise. Define the matrix $H = 4Q^T (\Sigma + \mu\mu^T) Q$. Then, H is symmetric and positive semi-definite because Σ and $\mu\mu^T$ both are positive semi-definite. Hence, H has non-negative eigenvalues. Furthermore, according to Lemma 8 in the appendix, \hat{H} converges to H as $m \rightarrow \infty$.

Theorem 4. Assume $k' \leq k$. Let $\lambda_1 \geq \dots \geq \lambda_n \geq 0$ be the eigenvalues of H , with corresponding orthogonal eigenvectors v_1, \dots, v_n . In particular, $\lambda_{k+1} = \dots = \lambda_n = 0$, as Q has rank k . Let $P_{k'}$ be the orthogonal projection onto the span of $v_1, \dots, v_{k'}$, that is,

$$P_{k'} = V_{k'} (V_{k'}^T V_{k'})^{-1} V_{k'}^T = V_{k'} V_{k'}^T,$$

where $V_{k'} = (v_1, \dots, v_{k'})$.

Assume $k' = n$ or $\lambda_{k'} > \lambda_{k'+1}$, referred to as the eigenvalue condition. Then, $\hat{P}_{k'} \rightarrow P_{k'}$ as $m \rightarrow \infty$. If the eigenvalue condition is fulfilled for $k' = k$, then $P_{k'} = P$, that is, P_k is the orthogonal projection onto the span of the row vectors of Q . In particular, the eigenvalue condition is fulfilled for $k' = k$ if and only if $\Sigma + \mu\mu^T$ is positive definite. The latter is the case if Σ is positive definite.

For $k' = k$, the correct row space of Q is found eventually, but not Q itself. If $k' < k$, then a subspace of this row space is found, corresponding to the k' largest eigenvalues. As the data is not mean centred, we discard the first principal component, and use the subsequent $k' - 1$ eigenvectors and eigenvalues.

Using PCA 2 (mean centred data) A popular approach to estimation of Π in the admixture model is PCA based on mean centred data, or mean and variance normalised data (Pritchard et al. 2000; Engelhardt and Stephens 2010; Patterson et al. 2006).

Let $G_1 = G - \frac{1}{n}GE = G(I - \frac{1}{n}E)$ be the SNP-wise mean centred genotypes, where E is an $n \times n$ matrix with all entries equal to one. Following the exposition and notation in Cabrer0s and Storey (2019), let $G_1 = U\Delta V^T$ be the SVD of G_1 , where ΔV^T consists of the row-wise principal components of G_1 , ordered according to the singular values. Define

$$S_{k'} = \begin{pmatrix} U_{1:(k'-1)}^T \\ e \end{pmatrix},$$

where $e = (1 \ 1 \ \dots \ 1)$ is a vector with all entries one, and $U_{1:(k'-1)}^T$ contains the top $k' - 1$ rows of U^T . Then, an estimate of the projection is

$$\hat{P}_{k'} = S_{k'}^T (S_{k'} S_{k'}^T)^{-1} S_{k'}.$$

The squared singular values in the SVD decomposition of G_1 are the same as the eigenvalues of

$$\hat{H}_1 = \frac{1}{m} G_1^T G_1 = \frac{1}{m} \left(I - \frac{1}{n} E \right) G^T G \left(I - \frac{1}{n} E \right)$$

(Jolliffe 2002). We have

$$\begin{aligned} \mathbb{E}[\hat{H}_1] &= \frac{1}{m} \left(I - \frac{1}{n} E \right) \mathbb{E}[G^T G] \left(I - \frac{1}{n} E \right) \\ &= \left(I - \frac{1}{n} E \right) (D + 4Q^T (\Sigma + \mu\mu^T) Q) \left(I - \frac{1}{n} E \right). \end{aligned} \quad (3)$$

Let H_1 denote the right hand side of (3).

Theorem 5. Let $\lambda_1 \geq \dots \geq \lambda_n$ be the eigenvalues of H_1 , with corresponding orthogonal eigenvectors v_1, \dots, v_n . In particular, $v_n = e$ and $\lambda_n = 0$. If D has all diagonal entries positive, then $\lambda_{n-1} > 0$.

Let $k' \leq n$ and let $P_{k'}$ be the orthogonal projection onto the span of $v_1, \dots, v_{k'-1}, e$, that is,

$$P_{k'} = V_{k'} (V_{k'}^T V_{k'})^{-1} V_{k'}^T,$$

where $V_{k'} = (v_1, \dots, v_{k'-1}, e)$. If $k' = n$ or $\lambda_{k'} > \lambda_{k'+1}$, then $\hat{P}_{k'} \rightarrow P_{k'}$ as $m \rightarrow \infty$.

There are no guarantees that for $k' = k$, we have $P_k = P$ and that the difference between \hat{B} and \hat{C} converges to zero for large m . However, this is the case under some extra conditions, and appears to be the case in many practical situations, see the Results section.

Theorem 6. Assume $D = dI$ for some $d > 0$. Furthermore, assume the vector e is in the row space of Q (this is, for example, the case if the admixture proportions sum to one for each individual). Then, $\lambda_k = \dots = \lambda_{n-1} = d$, and $\lambda_n = 0$.

If $\Sigma + \mu\mu^T$ is positive definite, then $\lambda_{k+1} > \lambda_k$ and $P_k = P$, where P_k is as in Theorem 4. As a consequence, with $k' = k$ in Theorem 1, $\hat{B} - \hat{C} \rightarrow 0$ as $m \rightarrow \infty$.

Using PCA 3 (mean and variance normalised data) Let $G_2 = W^{-1}G_1$ be the SNP mean and variance normalised genotypes, where W is an $m' \times m'$ diagonal matrix with s -th entry being the observed standard deviation of the genotypes of SNP s . All SNPs for which no variation are observed are removed, hence the number of SNPs might be smaller than the original number, $m' \leq m$. Following the same procedure as for PCA 2, let $G_2 = U\Delta V^T$ be the SVD of G_2 , where

ΔV^T consists of the row-wise principal components of G_2 , ordered according to the singular values. Define

$$S_{k'} = \begin{pmatrix} V_{1:(k'-1)}^T \\ e \end{pmatrix},$$

where $e = (1 \ 1 \ \dots \ 1)$, and $V_{1:(k'-1)}^T$ contains the top $k' - 1$ rows of V^T .

Then, an estimate of the projection is $\hat{P}_{k'} = S_{k'}^T (S_{k'} S_{k'}^T)^{-1} S_{k'}$.

We are not aware of any theoretical justification of this procedure similar to Theorem 1, but it appears to perform well in many practical situations, according to our simulations.

Simulation of genotype data

We simulated genotype data from different demographic scenarios using different sampling strategies. We deliberately choose different sampling strategies to challenge the method. We first made simple simulations that illustrate the problem of model fit as well as to demonstrate the theoretical and practical properties of the residual correlations that arise from having data from a finite number of individuals and a large number of SNPs. An overview of the simulations are given in Table 1.

In the first two scenarios, the ancestral allele frequencies are simulated independently for each ancestral population from a uniform distribution, $F_{si} \sim \text{Unif}(0, 1)$ for each site $s = 1, \dots, m$ and each ancestral population $i = 1, \dots, k$. In scenario 1, we simulated unadmixed individuals from three populations with either an equal or an unequal number of sampled individuals from each population. In scenario 2, we simulated two ancestral populations and a population that is admixed with half of its ancestry coming from each of the two ancestral populations.

In scenario 3, we set $F_{si} \sim \text{Unif}(0.01, 0.99)$ and simulated spatial admixture in a way that resembles a spatial decline of continuous gene flow between populations living in a long narrow island. We first simulated a single population in the middle of the long island. From both sides of the island, we then recursively simulated new populations from a Balding-Nichols distribution with parameter $F_{st} = 0.001$ using the R package 'bnpsd' (Ochoa and Storey 2019). In this way, each pair of adjacent populations along the island has an F_{st} of 0.001. Additional details on the simulation and an schematic visualization can be found in Figure 2 of Garcia-Erill and Albrechtsen (2020).

In scenario 4, we first simulated allele frequencies for an ancestral population from a symmetric beta distribution with shape parameter 0.03, $F_{si} \sim \text{Beta}(0.3, 0.3)$, which results in an allele frequency spectrum enriched for rare variants, mimicking the human allele frequency spectrum. We then sampled allele frequencies from a bifurcating tree (((pop1:0.1,popGhost:0.2):0.05,pop2:0.3):0.1,pop3:0.5), where pop1 and popGhost are sister populations and pop3 is an outgroup. Using the Balding-Nichols distribution and the F_{st} branch lengths of the tree (see Figure 5), we sampled allele frequencies in the four leaf nodes. Then, we created an admixed population with 30% ancestry from popGhost and 70% from pop2. We sampled 10 million genotypes for 50 individuals from each population except for the ghost population which was not included in the analysis, and subsequently removed sites with a sample minor allele frequency below 0.05, resulting in a total of 694,285 sites.

In scenario 5, we simulated an ancestral population with allele frequencies from a uniform distribution $F_{si} \sim \text{Unif}(0.05, 0.95)$, from which we sampled allele frequencies for two daughter populations from a Balding-Nichols distributions with $F_{st} = 0.3$ from the ancestral population, using 'bnpsd'. We then created recent hybrids based on a pedigree where all but one founder has ancestry from the first population. The number of generations in the pedigree then determines the admixture proportions and the age of the admixture where F1

individuals have one unadmixed parent from each population and backcross individuals have one unadmixed parent and the other F1. Double backcross individuals have one unadmixed parent and the other is a backcross. We continue to quadruple backcross with one unadmixed parent and the other triple backcross. Note that for the recent hybrids the ancestry of the pair of alleles at each loci is no longer independent which is a violation of the admixture model.

Results

Scenario 1

In this first set-up, we demonstrate the method using PCA 1 only. We simulated unadmixed individuals from $k = 3$ ancestral populations

$$Q = \begin{pmatrix} 1_{n_1} & 0 & 0 \\ 0 & 1_{n_2} & 0 \\ 0 & 0 & 1_{n_3} \end{pmatrix},$$

where 1_{n_i} is a row vector with all elements being one, and $n_1 + n_2 + n_3 = n$. We simulated genotypes for $n = 60$ individuals with sample sizes n_1, n_2 and n_3 , respectively, as detailed in the previous section. In Figure 1(A), we show the residual correlation coefficients for $k' = 2, 3$ and plot the corresponding major PCs. For the PCA 1 approach, the first principal component does not relate to population structure as the data is not mean centered, and we use the following $k' - 1$ principal components.

When assuming that there are only two populations, $k' = 2$, we note that the empirical correlation coefficients appear largely consistent within each population sample, but the corrected correlation coefficients are generally non-zero with different signs, which points to model misfit. In contrast, when assuming the correct number of populations is $k' = 3$, the empirical correlation coefficients match nicely the theoretical values of $-\frac{1}{n_i - 1}$, which comply with Theorem 2 (see Table 2). A fairly homogeneous pattern in the corrected correlation coefficients appears around zero across all samples. This is a good indication that the model fits well and that the PCA plots using principal components 2 and 3 reflex the data well.

Scenario 2

In this set-up we also include admixed individuals. We simulated samples from two ancestral populations and individuals that are a mix of the two. We then applied all three PCA procedures and the software ADMIXTURE to the data. Specifically, we choose

$$Q = \begin{pmatrix} 1_{n_1} & \frac{1}{2} 1_{n_2} & 0 \\ 0 & \frac{1}{2} 1_{n_2} & 1_{n_3} \end{pmatrix},$$

with $k = 2$ true ancestral populations, and $(n_1, n_2, n_3) = (20, 20, 20)$ or $(n_1, n_2, n_3) = (10, 20, 30)$, see the previous section for details. We analysed the data with $k' = 1, 2, 3$, and obtained the correlation structure shown in Figures 2 and 3, and Table 2. The two standard approaches PCA 2 and PCA 3 show almost identical results, hence only PCA 2 is shown in the figures. Both PCA 2 and PCA 3 use the top principal components, while PCA 1 disregards the first, hence the discrepancy in the axis labeling in Figures 2(b) and 3(b). For $k' = 1$ none of the principal components are used and the predicted normalized genotypes is simply 0. All four methods show consistent results, in particular, for the correct $k' (= 2)$, while there are smaller discrepancies between the methods for wrong $k' = 1, 3$. This is most pronounced for PCA 1 and ADMIXTURE. We note that the average correlation coefficient of \hat{b} within each population sample comply with Theorem 1 (see Table 2).

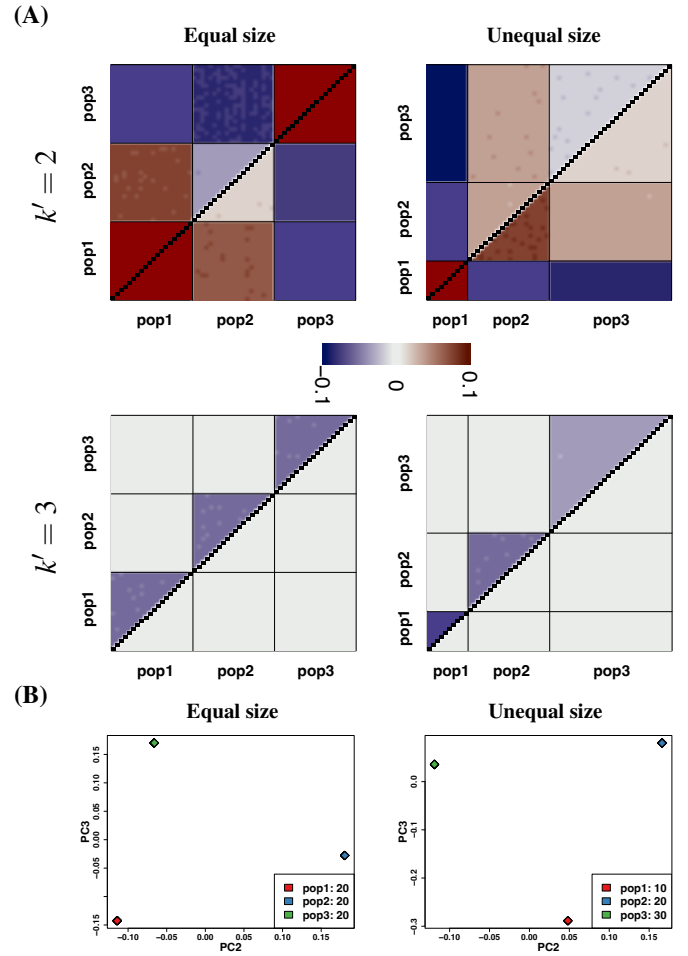


Figure 1 Results for simulated Scenario 1. (A) The upper triangle in the plots shows the empirical correlation coefficients \hat{b} and the lower triangle shows the corrected correlation coefficients $\hat{b} - \hat{c}$. (B) The major principal components ($k' = 3$) result in a clear separation of the three samples (all data points within each sample are almost identical).

A fairly homogeneous pattern in the corrected correlation coefficients appears around zero across all samples for $k' = 2$, as in scenario 1, which shows that the model fits well. However, unlike in scenario 1 the bias for the empirical correlation coefficient is not a simple function of the sample size (see Table 2).

In this case, and similarly in all other investigated cases, we don't find any big discrepancies between the four methods. Therefore, we only show the results of PCA 1 for which we have theoretical justification for the results.

Scenario 3

We simulated genotypes for $n = 500$ individuals at $m = 88,082$ sites with continuous genetic flow between individuals, thus there is not a true k . We analysed the data assuming $k' = 2, 3$, see Figure 4. In the figure, the individuals are ordered according to the estimated proportions of the ancestral populations, hence it appears there is a color wave pattern in the empirical and the corrected correlation coefficients, see Figure 4(A). As expected, the corrected correlation coefficients are closer to zero for $k' = 3$ than $k' = 2$, though the deviations from zero are still large. We thus find no support for the model for either value of k' . This is consistent with the plots of the major PCs, that show

Table 1 Overview of simulations.

Scenario	k	n	m	Description	F_{is}^a
1	3	20,20,20	500K	Unadmixed	Unif(0,1)
1	3	10,20,30	500K	Unadmixed	Unif(0,1)
2	2	20,20,20	500K	Admixed	Unif(0,1)
2	2	10,20,30	500K	Admixed	Unif(0,1)
3		500	100K ^b	Spatial with $F_{st} = 0.001$ between adjacent populations	Unif(0.01,0.99)
4	4	50,50,50,50,0 ^c	10M ^d	Ghost admixture	Beta(0.3,0.3)
5	2	20,20,50	500K	Recent hybrids	Unif(0.05,0.95)

^a Ancestral allele frequencies, $i = 1, \dots, k$ ^b after applying MAF > 5% filtering, 88,082 remained.^c No reference samples are provided on the ghost population.^d after applying MAF > 5% filtering, 694,285 remained.**Table 2** The mean (standard deviation) of \hat{b} and $\hat{b} - \hat{c}$ within each population using PCA 1.

Scenario 1	k'	n		pop1	pop2	pop3	
	3	(20, 20, 20)	\hat{b}^a	-0.0526 (0.0015)	-0.0526 (0.0016)	-0.0526 (0.0016)	
				-0.0526	-0.0526	-0.0526	
			$\hat{b} - \hat{c}$	0e-04 (0.0015)	0e-04 (0.0016)	0e-04 (0.0016)	
	(10, 20, 30)	\hat{b}	-0.1111 (0.0011)	-0.0526 (0.0016)	-0.0345 (0.0016)		
			-0.1111	-0.0526	-0.0345		
		$\hat{b} - \hat{c}$	0e-04 (0.0012)	0e-04 (0.0016)	0e-04 (0.0016)		
Scenario 2	k'	n		pop1	admixed	pop3	
	2	(20, 20, 20)	\hat{b}	-0.0419 (0.0015)	-0.0192 (0.0015)	-0.0420 (0.0015)	
				-0.0420	-0.0193	-0.0420	
			$\hat{b} - \hat{c}$	0e-04 (0.0015)	0e-04 (0.0015)	0e-04 (0.0015)	
	(10, 20, 30)	\hat{b}	-0.0701 (0.0018)	-0.0228 (0.0014)	-0.0304 (0.0016)		
			-0.0701	-0.0229	-0.0304		
		$\hat{b} - \hat{c}$	0e-04 (0.0017)	0e-04 (0.0014)	0e-04 (0.0016)		
Scenario 4	k'	n		pop1	pop2	pop3	pop4
	3	(50, 50, 50, 50)	\hat{b}	-0.0190 (0.0015)	0.0027 (0.0015)	-0.0204 (0.0017)	0.0122 (0.0013)
			$\hat{b} - \hat{c}$	0.0009 (0.0015)	0.0147 (0.0015)	0e-04 (0.0017)	0.0208 (0.0013)
	4	\hat{b}	-0.0204 (0.0015)	-0.0204 (0.0015)	-0.0204 (0.0017)	-0.0204 (0.0014)	
		$\hat{b} - \hat{c}$	0e-04 (0.0015)	0e-04 (0.0015)	0e-04 (0.0017)	0e-04 (0.0013)	

^a The second line of \hat{b} in each case shows the theoretical value obtained from the limit in Theorem 1.

continuous change without grouping the data into two or three clusters, see Figure 4(B).

Scenario 4

This case is based on the tree in Figure 5, which include an unsampled (so-called) ghost population, popGhost. The popGhost is sister population to pop1.

We simulated genotypes for $n = 200$ individuals: 150 unadmixed samples from pop1, pop2, and pop3; and 50 samples admixed with 0.3

ancestry from popGhost and 0.7 ancestry from pop2 (as pop4), as detailed in the previous section. As there is drift between the populations and hence genetic differences, the correct $k = 4$ (pop1, pop2, pop3, popGhost). This is picked up by our method that clearly shows $k' = 3$ is wrong with large deviation from zero in the corrected correlation coefficients. In contrast, for $k' = 4$, the corrected correlation coefficients are almost zero (Figure 6).

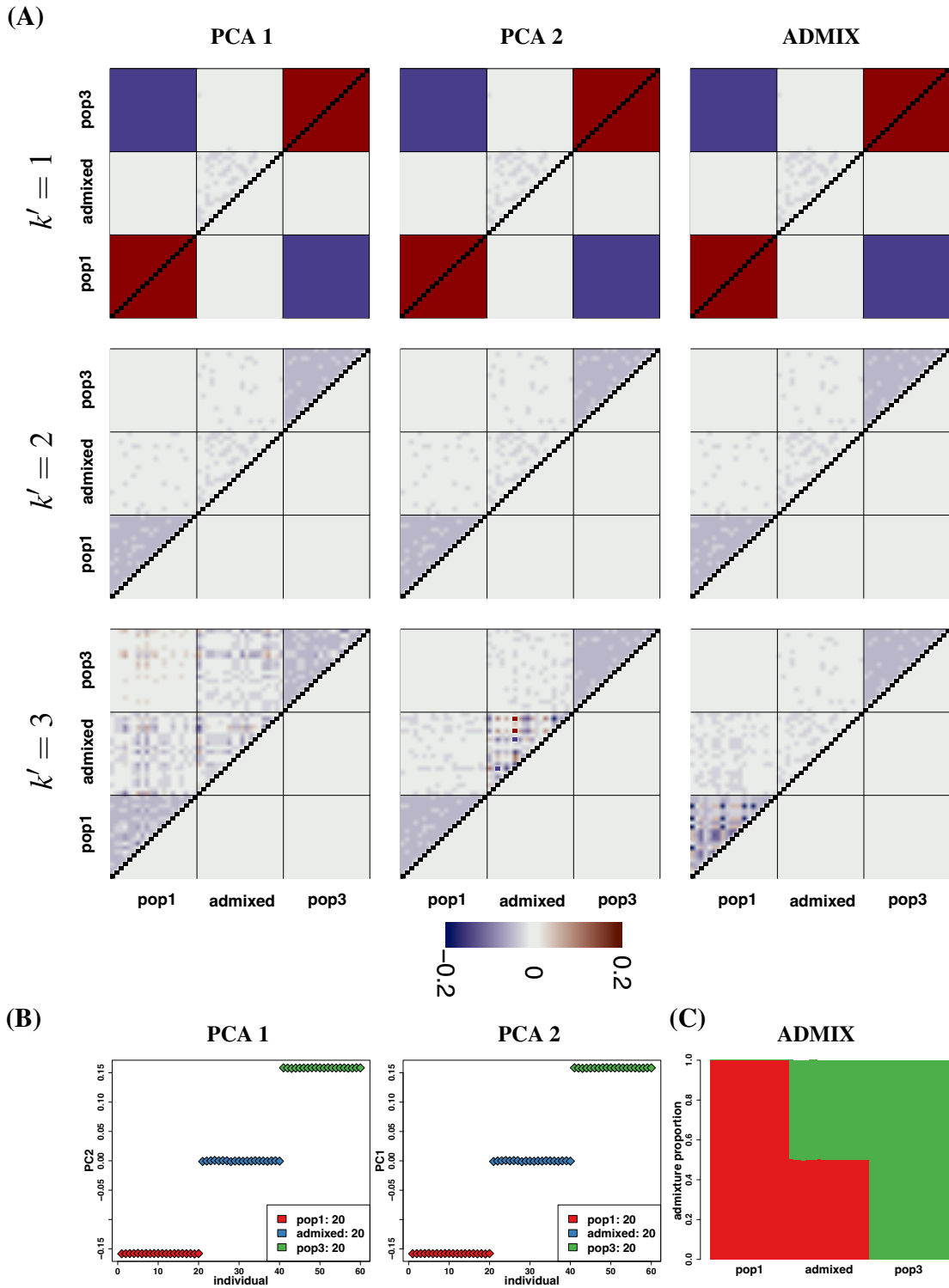


Figure 2 Results for simulated Scenario 2 with equal sample sizes. (A) For each of PCA 1, PCA 2 and ADMIXTURE, the upper left triangle in the plots shows the empirical correlation \hat{b} and the lower right triangle shows the difference $\hat{b} - \hat{c}$ with sample sizes $(n_1, n_2, n_3) = (20, 20, 20)$. (B) The major principal component for the PCA based methods for $k' = 2$ (in which case there is only one principal component). Individuals within each sample have the same color. (C) The estimated admixture proportions in the case of ADMIXTURE.

Scenario 5

In the last example, we simulated two populations (originating from a common ancestral population) and created admixed populations by backcrossing, as detailed in the previous section. Thus, the model does

not fulfil the assumptions of the admixture model in that the number of reference alleles are not binomially distributed, but depends on the particular backcross and the frequencies of the parental populations.

We simulate genotypes for $n = 90$ individuals at $m = 500,000$ sites.

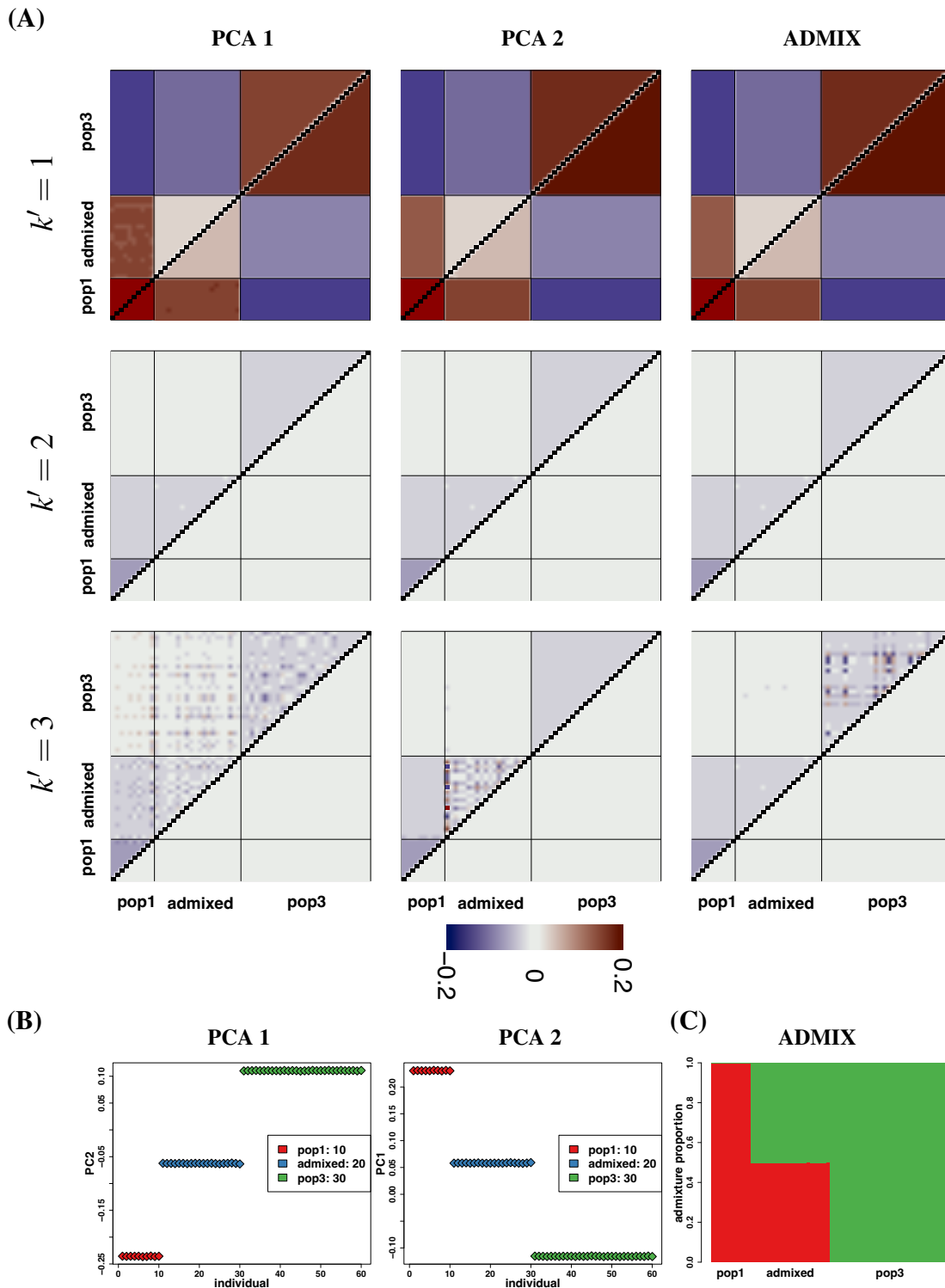


Figure 3 Results for simulated Scenario 2 with unequal sample sizes. (A) For each of PCA 1, PCA 2 and ADMIXTURE, the upper left triangle in the plots shows the empirical correlation \hat{b} and the lower right triangle shows the difference $\hat{b} - \hat{c}$ with sample sizes $(n_1, n_2, n_3) = (20, 20, 20)$. (B) The major principal component for the PCA based methods for $k' = 2$ (in which case there is only one principal component). Individuals within each sample have the same color. (C) The estimated admixture proportions in the case of ADMIXTURE.

There are 20 homogeneous individuals from each parental population, and 10 different individuals from each of the different recent admixture classes. Then, we analysed the data with $k' = 2$ and found the corrected correlation coefficients deviated consistently from zero, in particular

for one of the parental populations (Figure 7). We are thus able to say the admixture model does not provide a reasonable fit.

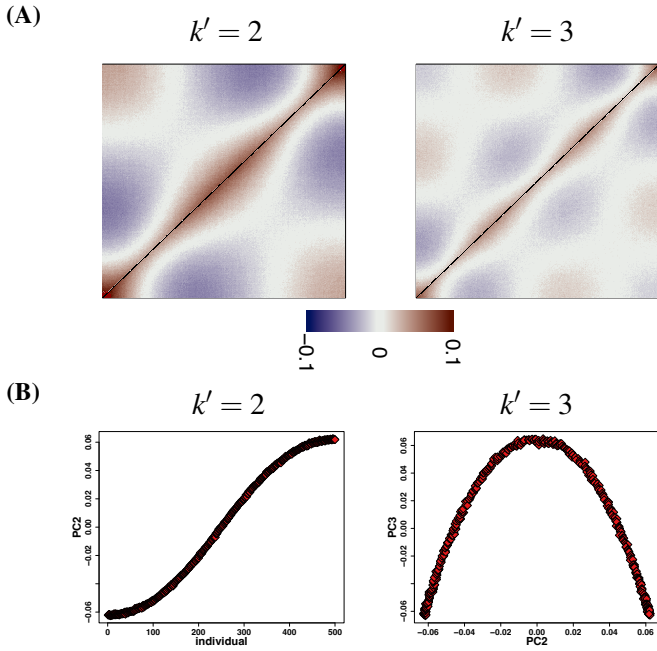


Figure 4 Results for simulated scenario 3. (A) The upper triangle in the plots shows the empirical correlation \hat{b} and the lower triangle shows the difference $\hat{b} - \hat{c}$. (B) The major principal components (only one in the case of $k' = 2$).

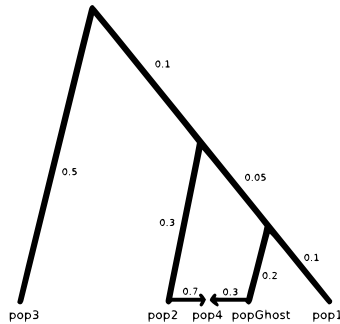


Figure 5 Schematic of the tree used to simulate population allele frequencies for Scenario 4, including 5 populations: pop1, pop2, pop3, pop4 and popGhost. The pop4 population is the result of admixture between pop2 and popGhost, for which there are no individuals sampled and is therefore a ghost population. The values in the branches indicate the drift in units of F_{ST} . The values along the two admixture edges are the admixture proportions coming from each population.

Real data

We analysed a whole genome sequencing data set from the 1000 Genomes Project (Auton *et al.* 2015), see also Garcia-Erill and Albrechtsen (2020) where the same data is used. It consists of data from five groups of different descent: a Yoruba group from Ibadan, Nigeria (YRI), residents from Southwest US with African ancestry (ASW), Utah residents with Northern and Western European ancestry (CEU), a group with Mexican ancestry from Los Angeles, California (MXL), and a group of Han Chinese from Beijing, China (CHB) with sample sizes 108,61,99,63 and 103, respectively, in total, $n = 434$. We kept only sites present in the Human Origins SNP panel (Lazaridis *et al.* 2014), with a total of $m = 406,279$ SNPs were left after a MAF filter of 0.05.

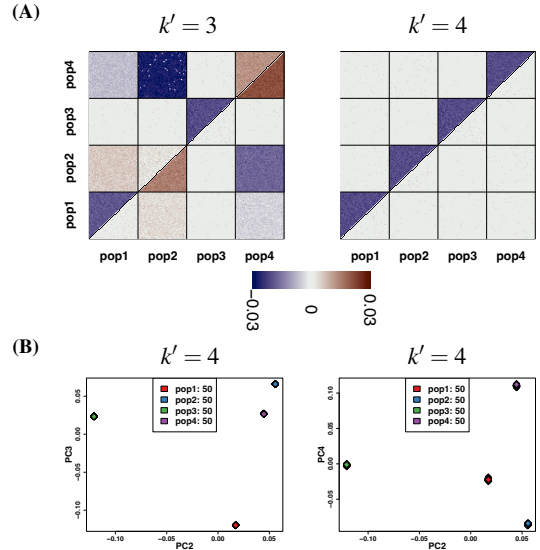


Figure 6 Results for simulated scenario 4. (A) The upper triangle in the plots shows the empirical correlation \hat{b} and the lower triangle shows the difference $\hat{b} - \hat{c}$. (B) The major principal components for $k' = 4$, that result in a clear separation of the four samples (all data points within each sample are almost identical).

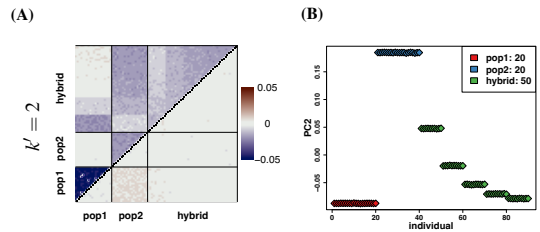


Figure 7 Results for simulated scenario 5 (recent admixture). (A) The upper triangle in the plots shows the empirical correlation \hat{b} and the lower triangle shows the difference $\hat{b} - \hat{c}$. (B) The major principal component for $k' = 2$.

We analyzed the data with $k' = 3, 4$. For $k' = 3$, Figure 8 shows that it is not possible to explain the relationship between MXL, CEU and CHB, indicating that MXL is not well explained as a mixture of the two. For $k' = 4$, the color shades of the corrected correlation coefficients are almost negligible within each population, pointing at a contribution from a native american population. This is further corroborated in Figure 8(D) that shows estimated proportions from the four ancestral populations using the software ADMIXTURE.

Discussion

We have developed a novel approach to assess model fit of PCA and the admixture model based on structure of the residual correlation matrix. We have shown that it performs well for simulated and real data, using a suit of different PCA methods, commonly used in the literature, and the ADMIXTURE software to estimate model parameters. By assessing the residual correlation structure visually, one is able to detect model misfit and violation of modelling assumptions.

The model fit is assessed by comparing visually two matrices of residual correlation coefficients. The theoretical and practical advantage of our approach lie in three aspects. First, our approach is computationally simple and fast. Calculation of the two residual correlation matrices and their difference is computationally inexpensive. Secondly,

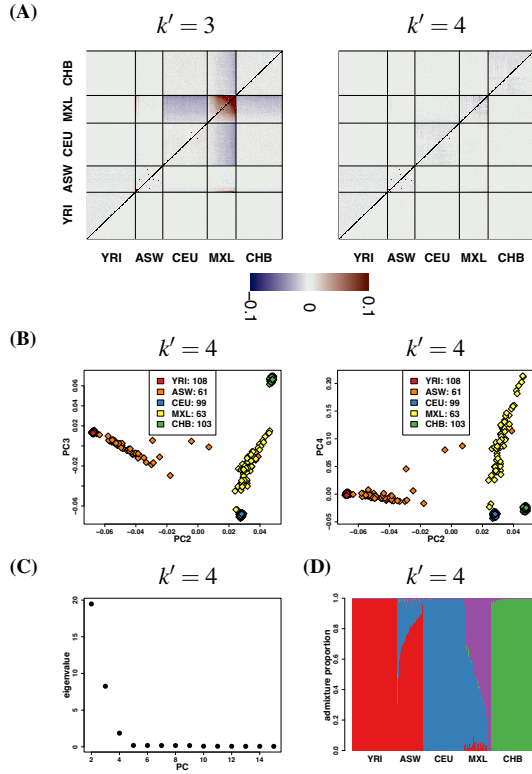


Figure 8 The residual correlation coefficient, the inferred population structure and the admixture proportions of a real human data from 1000 Genomes project. (A) The upper triangle in the plots shows the empirical correlation coefficient \hat{b} and the lower triangle shows the difference $\hat{b} - \hat{c}$. (B) The three major principal component for PCA 1 for $k' = 4$. (C) The eigenvalue for the first PC is removed and the eigenvalues corresponding to the remaining PCs are close to 0 after the fourth PC. (D) The admixture proportions as estimated with ADMIXTURE.

our approach provides a unified approach to model fitting based on PCA and clustering methods (like ADMIXTURE). In particular, it provides simple means to assess the adequacy of the chosen number of top principal components to describe the structure of the data. Assessing the adequacy by plotting the principal components against each other might lead to false confidence. In contrast, our approach exposes model misfit by plotting the difference between two matrices of the residual correlation coefficients. Thirdly, it comes with theoretical guarantees in some cases. These guarantees are further back up by simulations in cases, we cannot provide theoretical validity. Finally, our approach might be adapted to work on NGS data without estimating genotypes first, but working directly on genotype likelihoods.

Data availability

The data sets used in this study are all publicly available, including simulated and real data. Information about the R code used to analyze and simulate data is available at <https://github.com/Ginwaitthreebody/evalPCA>. The variant calls for the 1000 Genomes Project data used are publicly available at <ftp://ftp.1000genomes.ebi.ac.uk/vol1/ftp/release/20130502/>.

Acknowledgements

The authors are supported by the Independent Research Fund Denmark (grant number: 8021-00360B) and the University of Copenhagen through the Data+ initiative. SL acknowledges the financial support from the funding agency of China Scholarship Council. GGE and

AA are supported by the Independent Research Fund Denmark (grant numbers: 8049-00098B and DFF-0135-00211B respectively).

Appendix A

We first state the expectation and covariance matrix of G_{s^*} and Π_{s^*} , respectively, under the given distributional assumptions,

$$\mathbb{E}[\Pi_{s^*}] = \mu^T Q, \quad \text{cov}(\Pi_{s^*}) = Q^T \Sigma Q,$$

$$\mathbb{E}[G_{s^*}] = 2 \mathbb{E}[F_{s^*} Q] = 2\mu^T Q,$$

$$\text{cov}(G_{s^*}) = \mathbb{E}[\text{cov}(G_{s^*} | \Pi)] + 4 \text{cov}(\Pi_{s^*}) = D + 4Q^T \Sigma Q,$$

for $s = 1, \dots, m$, where

$$D = 2 \mathbb{E}[\text{diag}(\Pi_{s_1}(1 - \Pi_{s_1}), \dots, \Pi_{s_m}(1 - \Pi_{s_m}))],$$

and

$$\mathbb{E}[\Pi_{s_i}(1 - \Pi_{s_i})] = \mu^T Q_{*i} - (\mu^T Q_{*i})^2 - (Q^T \Sigma Q)_{ii}.$$

The unconditional columns G_{s^*} , $s = 1, \dots, m$, of G are independent random vectors by construction.

The above implies that

$$\frac{1}{m} \mathbb{E}[G^T G] = D + 4Q^T (\Sigma + \mu \mu^T) Q. \quad (4)$$

Auxiliary results are in appendix B.

Lemma 7. *The estimator \hat{D} is an unbiased estimator of D , that is, $\mathbb{E}[\hat{D}] = D$. Furthermore, it holds that $\hat{D} \rightarrow D$ as $m \rightarrow \infty$.*

Proof. Conditional on Π_{s_i} , using binomiality, we have $\mathbb{E}[G_{s_i}(2 - G_{s_i}) | \Pi_{s_i}] = 2\Pi_{s_i}(1 - \Pi_{s_i})$, and the first result follows. For convergence, note that $G_{s_i}(2 - G_{s_i})$, $s = 1, \dots, m$, unconditionally, form a sequence of iid random variables with finite variance, hence the convergence statement follows from the strong Law of Large Numbers (Jacod and Protter 2004). \square

Lemma 8. *The estimator $\hat{H} = \frac{1}{m} G^T G - \hat{D}$ is an unbiased estimator of $H = 4Q^T (\Sigma + \mu \mu^T) Q$, that is, $\mathbb{E}[\hat{H}] = H$. Furthermore, it holds that $\hat{H} \rightarrow 4Q^T (\Sigma + \mu \mu^T) Q$ as $m \rightarrow \infty$, and*

$$\mathbb{E} \left[\|\hat{H} - 4Q^T (\Sigma + \mu \mu^T) Q\|_F^2 \right] \leq \frac{16n^2}{m}.$$

Proof. Unbiasedness follows from (4) and Lemma 7. Consider the (i, j) -th entry of $\frac{1}{m} G^T G$, namely, $\frac{1}{m} \sum_{s=1}^m G_{s_i} G_{s_j}$. The sequence $G_{s_i} G_{s_j}$, $s = 1, \dots, m$, is iid with finite variance, hence $\frac{1}{m} G^T G$ converges to $\mathbb{E}[G^T G]$ as $m \rightarrow \infty$ by the strong Law of Large Numbers (Jacod and Protter 2004). Combined with Lemma 7 gives convergence of \hat{H} to H as $m \rightarrow \infty$.

It remains to prove the inequality. Define

$$A_{s,ij} = \begin{cases} G_{s_i} G_{s_j} - 4(Q^T (\Sigma + \mu \mu^T) Q)_{ij} & \text{if } i \neq j, \\ 2G_{s_i}(G_{s_i} - 1) - 4(Q^T (\Sigma + \mu \mu^T) Q)_{ii} & \text{if } i = j. \end{cases}$$

Then,

$$\begin{aligned} (\hat{H}_{ij} - \mathbb{E}[\hat{H}_{ij}])^2 &= \left(\frac{1}{m} \sum_{s=1}^m A_{s,ij} \right)^2 = \frac{1}{m^2} \sum_{s=1}^m \sum_{t=1}^m A_{s,ij} A_{t,ij}, \\ \|\hat{H} - \mathbb{E}[\hat{H}]\|_F^2 &= \frac{1}{m^2} \sum_{i=1}^n \sum_{j=1}^n \sum_{s=1}^m \sum_{t=1}^m A_{s,ij} A_{t,ij}. \end{aligned}$$

Using $\mathbb{E}[A_{s,ij}] = 0$, independence of $A_{s,ij}$ and $A_{t,ij}$ for $s \neq t$, and $|A_{s,ij}| \leq 4$, we have

$$\mathbb{E}[\|\hat{H} - \mathbb{E}[\hat{H}]\|_F^2] = \frac{1}{m^2} \sum_{i=1}^n \sum_{j=1}^n \sum_{s=1}^m \mathbb{E}[A_{s,ij}^2] \leq \frac{1}{m^2} 16mn^2 = \frac{16n^2}{m},$$

which proves the claim. \square

The convergence result is also in [Chen and Storey \(2015, theorem 2\)](#). The second part provides the rate of convergence of \hat{H} in the L^2 -norm. Convergence is contingent on large m , rather than large n , and requires m to increase at least like the square of n .

Proof of Theorem 1. Since $\hat{P}_{k'}$ is assumed to be an orthogonal projection, that is, $\hat{P}_{k'}^2 = \hat{P}_{k'}$ and $\hat{P}_{k'}^T = \hat{P}_{k'}$, then also the limit is an orthogonal projection, $P_{k'}^2 = P_{k'}$ and $P_{k'}^T = P_{k'}$.

Consider the empirical covariance \hat{B} . Define the variables $T_{k'} = G(I - P_{k'})$ with $\hat{P}_{k'}$ replaced by $P_{k'}$, and the empirical covariance

$$\begin{aligned}\tilde{B}_{ij} &= \frac{1}{m-1} \sum_{s=1}^m (T_{k',si} T_{k',sj} - \bar{T}_{k',i} \bar{T}_{k',j}) \\ &= \frac{1}{m-1} \sum_{s=1}^m T_{k',si} T_{k',sj} - \frac{m}{m-1} \bar{T}_{k',i} \bar{T}_{k',j},\end{aligned}$$

defined similarly to \hat{B}_{ij} , with $\bar{T}_{k',i} = \frac{1}{m} \sum_{s=1}^m T_{k',si}$. The sequences $T_{k',si} T_{k',sj}$, $s = 1, 2, \dots$, and $T_{k',si}$, $s = 1, 2, \dots$, are iid random variables, by the distributional assumptions on G . Furthermore, since $P_{k'}$ is an orthogonal projection, then $\|I - P_{k'}\|_F^2 \leq n$ is bounded ([Lemma 12](#)). Therefore, also $T_{k',si}$ is bounded uniformly in s, i by $2\sqrt{n} \leq 2n$.

Using boundedness, independence and the strong Law of Large Numbers ([Jacod and Protter 2004](#)),

$$\tilde{B}_{ij} \rightarrow \mathbb{E}[T_{k',1i} T_{k',1j}] - \mathbb{E}[T_{k',1i}] \mathbb{E}[T_{k',1j}] = \text{cov}(T_{k',1i}, T_{k',1j}), \quad (5)$$

for $m \rightarrow \infty$, and $\text{cov}(T_{k',1i}, T_{k',1j}) = (I - P_{k'})(D + 4Q^T \Sigma Q)(I - P_{k'})$. The latter equality follows from (4).

Consider $R = G(I - \hat{P}_{k'}) = G(I - P_{k'}) + G(P_{k'} - \hat{P}_{k'}) = T + G(P_{k'} - \hat{P}_{k'})$. Hence,

$$\begin{aligned}|\bar{R}_{k',i} - \bar{T}_{k',i}| &\leq \frac{1}{m} \sum_{s=1}^m \sum_{i'=1}^n \sum_{j'=1}^n 2|(P_{k'} - \hat{P}_{k'})_{i'j'}| \\ &= 2 \sum_{i'=1}^n \sum_{j'=1}^n |(P_{k'} - \hat{P}_{k'})_{i'j'}| \rightarrow 0,\end{aligned}$$

as $m \rightarrow \infty$ by assumption of the theorem. It follows that $\bar{R}_{k',i}$ converges to $\mathbb{E}[T_{k',1i}]$ as $m \rightarrow \infty$. Furthermore,

$$\begin{aligned}&\frac{1}{m-1} \sum_{s=1}^m R_{k',si} R_{k',sj} - \frac{1}{m-1} \sum_{s=1}^m T_{k',si} T_{k',sj} \\ &= \frac{1}{m-1} \sum_{s=1}^m (T_{si} + (G(P_{k'} - \hat{P}_{k'}))_{si})(T_{sj} + (G(P_{k'} - \hat{P}_{k'}))_{sj}) \\ &\quad - \frac{1}{m-1} \sum_{s=1}^m T_{k',si} T_{k',sj} \\ &= \frac{1}{m-1} \sum_{s=1}^m T_{si} (G(P_{k'} - \hat{P}_{k'}))_{sj} + \frac{1}{m-1} \sum_{s=1}^m (G(P_{k'} - \hat{P}_{k'}))_{si} T_{sj} \\ &\quad + \frac{1}{m-1} \sum_{s=1}^m (G(P_{k'} - \hat{P}_{k'}))_{si} (G(P_{k'} - \hat{P}_{k'}))_{sj}.\end{aligned}$$

The absolute value of the first term in the last line above is bounded by

$$\frac{4nm}{m-1} \sum_{j'=1}^n |(P_{k'} - \hat{P}_{k'})_{j'j'}|,$$

and similarly for the second term. The third is bounded by

$$\frac{4m}{m-1} \sum_{i'=1}^n \sum_{j'=1}^n |(P_{k'} - \hat{P}_{k'})_{i'i'}| |(P_{k'} - \hat{P}_{k'})_{j'j'}|.$$

All three terms converge to zero as $m \rightarrow \infty$, hence we conclude from (5) that $\hat{B}_{ij} \rightarrow \text{cov}(T_{k',1i}, T_{k',1j})$ as $m \rightarrow \infty$.

The result for the estimated covariance \hat{C} follows from convergence of \hat{D} and by assumption of the theorem. The remaining part follows from the convergence of \hat{B} and \hat{C} . Note that $QP = Q$, hence the second equation holds. The last statement of the theorem follows directly.

Proof of Theorem 2. Consider $T_k = G(I - P_k) = G(1 - P)$, where $P = Q^T(QQ^T)^{-1}Q$ is the projection onto the row space of Q . Then, T_k contains the residuals under multiple regression of the m rows of G on the k rows of Q ([Box et al. 2005](#)). Since e is in the row space of Q , then the sum of the residuals is zero for each $s = 1, \dots, m$: $\sum_{i=1}^n T_{k,si} = 0$ (the assumption that e is in the row space is equivalent to having an intercept in the regression model) ([Box et al. 2005](#)). We have, for $s = 1, \dots, m$,

$$\begin{aligned}0 &= \text{var} \left(\sum_{i=1}^n T_{k,si} \right) = \sum_{i=1}^n \text{var}(T_{k,si}) + \sum_{i=1}^n \sum_{j=1, i \neq j}^n \text{cov}(T_{k,si}, T_{k,sj}) \\ &= \sum_{i=1}^n \text{var}(T_{k,1i}) + \sum_{i=1}^n \sum_{j=1, i \neq j}^n \text{cov}(T_{k,1i}, T_{k,1j}),\end{aligned}$$

since the distribution of $T_{k,si}$ is independent of s . From the proof of [Theorem 4](#), it follows that \hat{B} converges to $\text{cov}(T_{k,1\star})$ as $m \rightarrow \infty$. Hence,

$$\sum_{i=1}^n \hat{B}_{ii} + \sum_{i=1}^n \sum_{j=1, i \neq j}^n \hat{B}_{ij} \rightarrow 0, \quad \text{as } m \rightarrow \infty,$$

and the desired result follows by rearrangement.

If Q takes the given form, then the residuals under multiple regression are independent between compartments, as the projection is

$$P = \begin{pmatrix} P_1 & 0 & \cdots & 0 \\ 0 & P_2 & \cdots & 0 \\ \vdots & \vdots & \ddots & \vdots \\ 0 & 0 & \cdots & P_r \end{pmatrix},$$

where $P_\ell = Q_\ell^T(Q_\ell Q_\ell^T)^{-1}Q_\ell$ has dimension $n_\ell \times n_\ell$. It follows that the computation above holds for each compartment. Finally, if $Q_\ell = (1 \dots 1)$, then the distribution of the random vector $T_{k,1\star}$ is exchangeable, resulting in

$$\begin{aligned}0 &= \text{var} \left(\sum_{i=1}^{n_\ell} T_{k,1i} \right) = \sum_{i=1}^{n_\ell} \text{var}(T_{k,1i}) + \sum_{i=1}^{n_\ell} \sum_{j=1, i \neq j}^{n_\ell} \text{cov}(T_{k,1i}, T_{k,1j}) \\ &= n_\ell \text{var}(T_{k,11}) + n_\ell(n_\ell - 1) \text{cov}(T_{k,11}, T_{k,12})\end{aligned}$$

assuming the individuals in the ℓ -th compartment are numbered 1 to n_ℓ . Rearranging terms and substituting \hat{b}_{ij} for the moments of $T_{k,i\star}$ yields the desired result.

Proof of Theorem 3. Consider $T_k = G(I - P_k) = G(1 - P)$, where $P = Q^T(QQ^T)^{-1}Q$ is the projection onto the row space of Q . If $Q_1 = (1 \dots 1)$, then the distribution of the random variables $T_{k,11}, \dots, T_{k,1n_1}$ are exchangeable, resulting in

$$\begin{aligned}0 &\leq \text{var} \left(\sum_{i=1}^{n_1} T_{k,1i} \right) = \sum_{i=1}^{n_1} \text{var}(T_{k,1i}) + \sum_{i=1}^{n_1} \sum_{j=1, i \neq j}^{n_1} \text{cov}(T_{k,1i}, T_{k,1j}) \\ &= n_1 \text{var}(T_{k,11}) + n_1(n_1 - 1) \text{cov}(T_{k,11}, T_{k,12}).\end{aligned}$$

Rearranging terms and substituting \hat{b}_{ij} for the moments of $T_{k,i\star}$ yields the desired result.

Proof of Theorem 4. The convergence statement of the theorem is a special case of [Theorem 9](#) in [Appendix B](#). Take $A_m = \hat{H}$ (that depends

on the number of SNPs m , and the particular realization), $A = H$, and $k = k'$ in the theorem (k is used as a generic index in Theorem 9). Then, $E_k E_k^T = P_{k'}$ and $F_{m,k} F_{m,k}^T = \hat{P}_{k'}$, and the conclusion of Theorem 4 holds. Convergence in Frobenius norm is equivalent to pointwise convergence (as n is fixed) $\hat{P}_{k'} \rightarrow P_{k'}$ as $m \rightarrow \infty$ by definition.

If $\Sigma + \mu\mu^T$ is positive definite, then it has rank k . As $\text{rank}(Q) = k$ by assumption, it follows from Lemma 13 that $\text{rank}(H) = k$. Consequently, there are k positive eigenvalues of H and $\lambda_{k+1} = 0$, and the eigenvalue condition holds. Conversely, assume the eigenvalue condition holds. By definition $\text{rank}(H) \leq k$. As $\lambda_k > \lambda_{k+1} \geq 0$ by assumption, then also $\text{rank}(H) \geq k$ and we conclude $\text{rank}(H) = k$. It follows that the rank of $\Sigma + \mu\mu^T$ is k ; consequently, it is positive definite.

If $k' = k = n$, then $P_k = V_k V_k^T = I$ and $P = I$ (as $k = n$), and $P_k = P$. So assume $k' = k < n$. Since the eigenvalue condition is fulfilled, then from the above, we have $\text{rank}(Q^T(\Sigma + \mu\mu^T)) = k$, and Lemma 13 yields that the row space of H and Q agree. Similarly, we have $H = V_k \text{diag}(\lambda_1, \dots, \lambda_k) V_k^T$ and Lemma 13 yields that the row space of H and V_k^T agree. This implies the row space of Q and V_k^T agree. Consequently, $P_k = Q^T(QQ^T)^{-1}Q = P$, and the statement holds.

Proof of Theorem 5. It follows trivially that e is an eigenvector of H_1 with eigenvalue 0. If D has all entries positive, then it is positive definite and $D + 4Q^T(\Sigma + \mu\mu^T)Q$ is also positive definite, hence has rank n . It follows from Lemma 13 that H_1 has rank $n - 1$, hence $\lambda_{n-1} > 0$.

Similarly to the proof of Lemma 8 in Appendix B, one can show $\mathbb{E}[\hat{H}_1] = H_1$ and $\hat{H}_1 \rightarrow H_1$ as $m \rightarrow \infty$, where H_1 denotes the right hand side of (3). The remaining part of the theorem is proven similarly to Theorem 4.

Proof of Theorem 6. Note that e is an eigenvector of H_1 with eigenvalue 0. Consider an eigenvector v of H_1 , orthogonal to e with eigenvalue λ . Then, the following two equations are equivalent,

$$\begin{aligned} \left(I - \frac{1}{n}E\right) (D + 4Q^T(\Sigma + \mu\mu^T)Q) \left(I - \frac{1}{n}E\right) v &= \lambda v, \\ 4 \left(I - \frac{1}{n}E\right) Q^T(\Sigma + \mu\mu^T)Q \left(I - \frac{1}{n}E\right) v &= (\lambda - d)v, \end{aligned} \quad (6)$$

where it is used that $D = dI$ and $v \perp e$. It shows that v is an eigenvector of $K = 4(I - \frac{1}{n}E)Q^T(\Sigma + \mu\mu^T)Q(I - \frac{1}{n}E)$ with eigenvalue $\mu = \lambda - d$. Since Q has rank k and the vector e is in the space spanned by the rows of Q , then $Q(I - \frac{1}{n}E)$ has rank $k - 1$. It follows that there are at most $k - 1$ positive eigenvalues of K , that is, at most $k - 1$ eigenvalues of H_1 such that $\lambda > d$. Furthermore, there are precisely $k - 1$ positive eigenvalues, provided $\Sigma + \mu\mu^T$ is positive definite (Lemma 13). The remaining eigenvalues of K are zero, that is, the corresponding eigenvalues of H_1 are $\lambda = d$.

Assume $\Sigma + \mu\mu^T$ is positive definite, then by the above argument there precisely are $k - 1$ eigenvalues of H_1 such that $\lambda > d$ with corresponding orthogonal eigenvectors v_1, \dots, v_{k-1} . It follows from (6) that v_1, \dots, v_{k-1} are in the space spanned by the rows of $Q(I - \frac{1}{n}E)$, hence the eigenvectors are in the space spanned by the rows of Q . By assumption e is also in that row span. Hence, v_1, \dots, v_{k-1}, e forms an orthogonal basis of the row span of Q , as Q has rank k . Thus, $P_k = P$.

Appendix B

Theorem 9. Let A_m be a sequence of symmetric $n \times n$ -matrices that converges to a symmetric $n \times n$ -matrix A in the Frobenius norm, that is $\|A_m - A\|_F \rightarrow 0$, as $m \rightarrow \infty$. Let $\lambda_1 \geq \dots \geq \lambda_n$ be the eigenvalues of A (with multiplicity, and not necessarily non-negative). Let $k \leq n$ be given

and assume either $k = n$ or $\lambda_k > \lambda_{k+1}$. Furthermore, let e_1, \dots, e_k be orthogonal eigenvectors corresponding to the eigenvalues $\lambda_1, \dots, \lambda_k$, respectively, and let $f_{m,1}, \dots, f_{m,k}$ be orthogonal eigenvectors corresponding to the k largest eigenvalues of A_m (with multiplicity). Then, the orthogonal projection onto the span of $f_{m,1}, \dots, f_{m,k}$ converges to the orthogonal projection onto the span of e_1, \dots, e_k in the Frobenius norm. That is, define $E_k = (e_1, \dots, e_k)$ and $F_{m,k} = (f_{m,1}, \dots, f_{m,k})$, then $\|F_{m,k} F_{m,k}^T - E_k E_k^T\|_F \rightarrow 0$ as $m \rightarrow \infty$.

Proof. If $k = n$, then $E_n E_n^T = I$ and $F_{m,n} F_{m,n}^T = I$, and the statement is trivial. Hence, assume $k < n$. Let e_1, \dots, e_n be eigenvectors of A corresponding to eigenvalues $\lambda_1, \dots, \lambda_n$, respectively. Let $f_{m,1}, \dots, f_{m,n}$ be the eigenvectors of A_m corresponding to the eigenvalues $\mu_{m,1} \geq \dots \geq \mu_{m,n}$. All eigenvectors can be assumed to be orthonormal.

As $\|A - A_m\|_F^2 \rightarrow 0$ for $m \rightarrow \infty$, then every entry of A_m converges to the corresponding entry of A . Consequently, the characteristic function of A_m converges to that of A , and the eigenvalues of A_m converges to those of A , that is, $\mu_{m,j} \rightarrow \lambda_j$ for $j = 1, \dots, n$, and $m \rightarrow \infty$. Let T_m be such that $E_n = F_{m,n} T_m$. As E_n and $F_{m,n}$ are orthogonal matrices, hence also T_m is orthogonal. Applying Lemma 10 in the first and third line gives

$$\begin{aligned} \|A - A_m\|_F^2 &= \|AE - A_m E_n\|_F^2 = \|E \text{diag}(\lambda_1, \dots, \lambda_n) - A_m F_{m,n} T_m\|_F^2 \\ &= \|F_{m,n} T_m \text{diag}(\lambda_1, \dots, \lambda_n) - F_{m,n} \text{diag}(\mu_{m,1}, \dots, \mu_{m,n}) T_m\|_F^2 \\ &= \|T_m \text{diag}(\lambda_1, \dots, \lambda_n) - \text{diag}(\mu_{m,1}, \dots, \mu_{m,n}) T_m\|_F^2 \\ &= \sum_{i=1}^n \sum_{j=1}^n (\lambda_j T_{m,ij} - \mu_{m,i} T_{m,ij})^2 = \sum_{i=1}^n \sum_{j=1}^n T_{m,ij}^2 (\lambda_j - \mu_{m,i})^2. \end{aligned}$$

By assumption, $\lambda_k > \lambda_{k+1}$. Hence, by convergence of eigenvalues, for $j \leq k$, $i \geq k + 1$, or $j \geq k + 1$, $i \leq k$, we have $T_{m,ij} \rightarrow 0$ as $m \rightarrow \infty$.

Furthermore,

$$\begin{aligned} E_k E_k^T - F_{m,k} F_{m,k}^T &= \sum_{\ell=1}^k (e_\ell e_\ell^T - f_{m,\ell} f_{m,\ell}^T) \\ &= \sum_{\ell=1}^k \left(\left(\sum_{a=1}^n f_{m,a} T_{m,a\ell} \right) \left(\sum_{a=1}^n f_{m,a} T_{m,a\ell} \right)^T - f_{m,\ell} f_{m,\ell}^T \right) \\ &= \sum_{\ell=1}^k \left(\sum_{a=1}^n \sum_{b=1}^n T_{m,a\ell} T_{m,b\ell} f_{m,a} f_{m,b}^T - f_{m,\ell} f_{m,\ell}^T \right) \\ &= \sum_{a=1}^n \sum_{b=1}^n \sum_{\ell=1}^k T_{m,a\ell} T_{m,b\ell} f_{m,a} f_{m,b}^T - \sum_{\ell=1}^k f_{m,\ell} f_{m,\ell}^T \\ &= \sum_{(a,b) \in \{1, \dots, n\}^2 \setminus A_{1,k}} \left(\sum_{i=1}^k T_{m,ai} T_{m,bi} \right) f_{m,a} f_{m,b}^T \\ &\quad + \sum_{(a,a) \in A_{1,k}} \left(\sum_{i=1}^k T_{m,ai} T_{m,ai} - 1 \right) f_{m,a} f_{m,a}^T, \end{aligned}$$

where $A_{i,j} = \{(a, a) : i \leq a \leq j\}$.

From Lemma 11, we have $f_{m,a} f_{m,b}^T \perp f_{m,c} f_{m,d}^T$ for $(a, b) \neq (c, d)$ in the Frobenius inner product. Moreover, $\|f_{m,a} f_{m,b}^T\|_F = 1$ for all a, b . Hence,

$$\begin{aligned} \|E_k E_k^T - F_{m,k} F_{m,k}^T\|_F^2 &= \sum_{(a,b) \in \{1, \dots, n\}^2 \setminus A_{1,k}} \left(\sum_{i=1}^k T_{m,ai} T_{m,bi} \right)^2 + \sum_{(a,a) \in A_{1,k}} \left(\sum_{i=1}^k T_{m,ai} T_{m,ai} - 1 \right)^2 \\ &= \sum_{(a,b) \in \{1, \dots, n\}^2 \setminus A_{1,n}} \left(\sum_{i=1}^k T_{m,ai} T_{m,bi} \right)^2 + \sum_{(a,a) \in A_{k+1,n}} \left(\sum_{i=1}^k T_{m,ai} T_{m,ai} \right)^2 \\ &\quad + \sum_{(a,a) \in A_{1,k}} \left(\sum_{i=1}^k T_{m,ai} T_{m,ai} - 1 \right)^2. \end{aligned} \quad (7)$$

As noted above, $T_{m,ij} \rightarrow 0$ as $m \rightarrow \infty$ for $j \leq k, i \geq k+1$, or $j \geq k+1, i \leq k$. Using this and orthogonality of T_m gives

$$\sum_{i=1}^k T_{m,ai} T_{m,bi} = \sum_{i=1}^n T_{m,ai} T_{m,bi} - \sum_{i=k+1}^n T_{m,ai} T_{m,bi} \rightarrow \begin{cases} 0 & \text{if } a \neq b, \\ 1 & \text{if } a = b, \end{cases}$$

Inserting into (7) results in $\|E_k E_k^T - F_{m,k} F_{m,k}^T\|_F^2 \rightarrow 0$, as $m \rightarrow \infty$. \square

Lemma 10. *Let A be an $a \times b$ matrix. Let U be a $b \times b$ orthogonal matrix and V an $a \times a$ orthogonal matrix. Then,*

$$\|A\|_F = \|VA\|_F = \|AU\|_F = \|VAU\|_F.$$

Proof. See Golub and Loan (2013). \square

Lemma 11. *Let $w, x, y, z \in \mathbb{R}^b$. For $a \times b$ -matrices A and B , let $\langle A, B \rangle_F = \sum_{i=1}^a \sum_{j=1}^b A_{ij} B_{ij}$ be the Frobenius inner product of A and B , and let $\langle \cdot, \cdot \rangle$ be the standard inner product on \mathbb{R}^b . Then, $\langle wx^T, yz^T \rangle_F = \langle w, y \rangle \langle x, z \rangle$. In particular, $\|wx^T\|_F = \|w\|_2 \|x\|_2$ and $wx^T \perp yz^T$ if $w \perp y$ or $x \perp z$.*

Proof. Note that

$$\langle wx^T, yz^T \rangle = \sum_{i=1}^b \sum_{j=1}^b w_i x_j y_i z_j = \sum_{i=1}^b w_i y_i \sum_{j=1}^b x_j z_j = \langle w, y \rangle \langle x, z \rangle.$$

Hence, if either $w \perp y$ or $x \perp z$, then $wx^T \perp yz^T$, and $\|wx^T\|_F^2 = \langle wx^T, wx^T \rangle = \langle w, w \rangle \langle x, x \rangle = \|w\|_2^2 \|x\|_2^2$, such that $\|wx^T\|_F = \|w\|_2 \|x\|_2$. \square

Lemma 12. *Let v_1, \dots, v_ℓ be linearly independent vectors. An orthogonal projection matrix on $\text{span}(v_1, \dots, v_\ell)$ has Frobenius norm $\sqrt{\ell}$.*

Proof. We may assume that v_1, \dots, v_ℓ are orthonormal. Then, we can write the projection matrix as $P = v_1 v_1^T + \dots + v_\ell v_\ell^T$. By Lemma 11, $v_i v_i^T \perp v_j v_j^T$ for $i \neq j$. So, again by Lemma 11, $\|P\|_F^2 = \|v_1 v_1^T\|_F^2 + \dots + \|v_\ell v_\ell^T\|_F^2 = \ell$. \square

Lemma 13. *Let A be an $a \times b$ matrix and B an $b \times c$ matrix, both of rank b , such that $a, c \geq b$. Let $C = AB$. Then, C is of rank b , and the row space of C coincides with the row space of B .*

Proof. First we show that $\text{rank}(C) = b$. Note that A has b linearly independent rows $1 \leq i_1 < \dots < i_b \leq b$, and B has b linearly independent columns $1 \leq j_1 < \dots < j_b \leq c$. Let \tilde{A} and \tilde{B} be the $b \times b$ matrices with $\tilde{A}_{cd} = A_{i_c d}$ and $\tilde{B}_{cd} = B_{c j_d}$. Then \tilde{A} and \tilde{B} are invertible matrices. Hence, also $\tilde{C} = \tilde{A}\tilde{B} = (C_{i_a j_b})_{a,b}$ is invertible and has rank k . It follows that C has rank k . As \tilde{A} is invertible, then the span of the rows of $\tilde{A}\tilde{B}$ is equal to the span of the rows of \tilde{B} . That is, the span of the rows of AB is equal to the span of the rows of B . \square

Literature cited

Alexander DH, Lange K. 2011. Enhancement of the admixture algorithm for individual ancestry estimation. *BMC Bioinformatics*. 12:246.
 Alexander DH, Novembre J, Lange K. 2009. Fast model-based estimation of ancestry in unrelated individuals. *Genome Res*. 19:1655–1664.
 Auton A, Brooks LD, Durbin RM, Garrison EP, Kang HM, Korbel JO, Marchini JL, McCarthy S, McVean GA, Abecasis GR *et al.* 2015. A global reference for human genetic variation. *Nature*. 526:68–74.

Balding DJ, Nichols RA. 1995. A method for quantifying differentiation between populations at multi-allelic loci and its implications for investigating identity and paternity. *Genetica*. 96:3–12.
 Box G, Hunter J, Hunter W. 2005. *Statistics for Experimenters: Design, Innovation, and Discovery*. Wiley Series in Probability and Statistics. Wiley.
 Cabrerós I, Storey J. 2019. A Likelihood-Free Estimator of Population Structure Bridging Admixture Models and Principal Components Analysis. *Genetics*. 212:1009–1029.
 Chen X, Storey J. 2015. Consistent estimation of low-dimensional latent structure in high-dimensional data.
 Conomos M, Reiner A, Weir B, Thornton T. 2016. Model-free estimation of recent genetic relatedness. *Am J Hum Genet*. 98:127–148.
 Engelhardt B, Stephens M. 2010. Analysis of population structure: a unifying framework and novel methods based on sparse factor analysis. *PLoS Genetics*. 6.
 Evanno G, Regaut S, Goudet J. 2005. Detecting the number of clusters of individuals using the software structure: A simulation study. *Mol Ecol*. 14:2622–2620.
 Garcia-Erill G, Albrechtsen A. 2020. Evaluation of model fit of inferred admixture proportions. *Molecular Ecology Resources*. 20:936–949.
 Golub GH, Loan CF. 2013. *Matrix Computations*. Johns Hopkins Studies in Mathematical Sciences. JHU Press.
 Jacod J, Protter P. 2004. *Probability Essentials*. Universitext. Springer.
 Janes JK, Miller JM, Dupuis JR, Malenfant RM, Gorrell JC, Cullingham CI, Andrew RL. 2017. The $k02$ conundrum. *Mol Ecol*. 26:3594–3602.
 Jolliffe IT. 2002. *Principle Component Analysis (2nd Ed.)*. Springer Series in Statistics. Springer.
 Jolliffe T, Cadima J. 2016. Principal component analysis: a review and recent developments. *Phil. Trans. R. Soc. A*. 374:0150202.
 Lawson D, van Dorp L, Falush D. 2018a. A tutorial on how not to over-interpret structure and admixture bar plots. *Nature Communications*. 9.
 Lawson DJ, van Dorp L, Falush D. 2018b. A tutorial on how not to over-interpret structure and admixture bar plots. *Nat Comm*. 19:3258.
 Lazaridis I, Patterson N, Mittnik A, Renaud G, Mallick S, Kirsanow K, Sudmant PH, Schraiber JG, Castellano S, Lipson M *et al.* 2014. Ancient human genomes suggest three ancestral populations for present-day Europeans. *Nature*. 513:409–413.
 Meisner J, Liu S, Huang M, Albrechtsen A. 2021. Large-scale inference of population structure in presence of missingness using PCA. *Bioinformatics*. 37:1868–1875.
 Ochoa A, Storey JD. 2019. f_{ST} and kinship for arbitrary population structures i: Generalized definitions. *bioRxiv*.
 Patterson N, Price AL, Reich D. 2006. Population structure and eigenanalysis. *PLoS Genetics*. 2:e190.
 Pickrell J, Pritchard J. 2012. Inference of population splits and mixtures from genome-wide allele frequency data. *PLoS Genetics*. 8:1–17.
 Pritchard J, Stephens M, Donnelly P. 2000. Inference of population structure using multilocus genotype data. *Genetics*. 155:945–959.
 Raj A, Stephens M, Pritchard J. 2014. Faststructure: Variational inference of populations structure in large snp data sets. *Genetics*. 197:573–589.
 Wang J. 2003. Maximum-likelihood estimation of admixture proportions from genetic data. *Genetics*. 154:747–765.
 Wang J. 2019. A parsimony estimator of the number of populations from a structure-like analysis. *Mol Ecol Res*. 19:970–981.